



Soon Yung Jun

Department of Physics
Carnegie Mellon University
Pittsburgh, PA 53210 USA

*for
the CDF Collaboration*

Hot topics in flavor physics at CDF are reviewed. Selected results of top, beauty, charm physics and exotic states in about 200 pb^{-1} data collected by the CDF II detector in $p\bar{p}$ collisions at $\sqrt{s} = 1.96 \text{ TeV}$ at the Fermilab Tevatron are presented.

1 Introduction

The upgraded Collider Detector at Fermilab (CDF) has collected around 450 pb^{-1} between February 2002 and August 2004 during the Tevatron Run II at Fermilab. With successful implementation of new triggers and fast electronics, the CDF II detector is able to accumulate a large statistics of physics-enriched samples for top, beauty and charm physics as well as to search for new physics. We present selected recent results in flavor physics from CDF.

2 Top Physics

The properties of the top quark play an important role in the Standard Model (SM) and in searches for new physics. The top quark is the only fermion near the electroweak scale. The top mass along with the measured W boson mass constraint on the mass of the Higgs particle. In the SM, the top quark decays almost exclusively into a W boson and a b -quark. Depending on decay of the W (leptonic or hadronic), there are three main categories of top pair production: dilepton, lepton+jets and all hadronic channels. In this section, selected results on the $t\bar{t}$ production cross section, the top mass measurement and the single top search are briefly described.

2.1 Production cross section

CDF measures the $t\bar{t}$ production cross section in all three W decay modes either by counting experiments or by fitting the data to kinematic distributions that can discriminate between signal and background. The result shown in Fig. 1 (Left) is based on using a kinematic fit to the leading transverse of energy (E_T) of the jet in the lepton+jet sample from 162 pb^{-1} data. Data are fitted to Monte Carlo derived template distributions for signal and that derived from

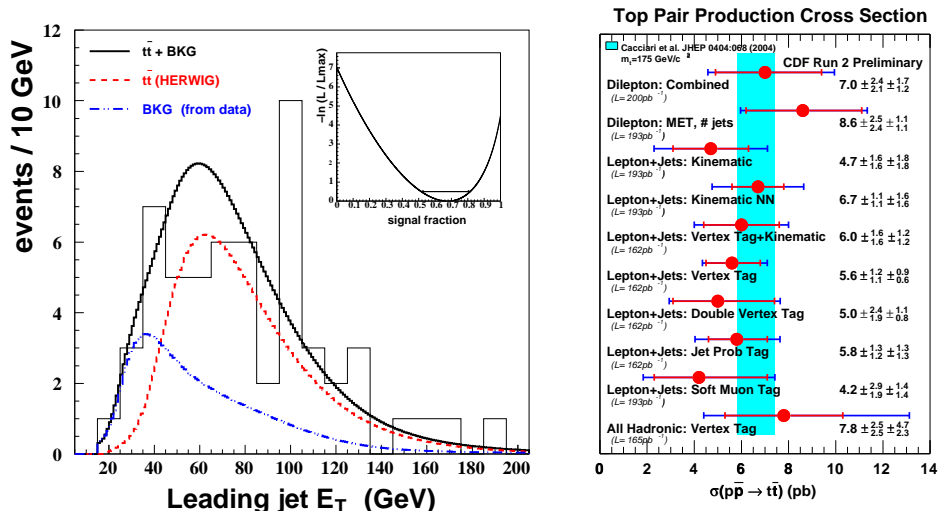


Figure 1: (Left) The leading jet E_T distribution with best fit curve in the signal region ($W+3$, or more jets). Two components fit using the shape of the $t\bar{t}$ signal (red) and that of the background (blue) provided $0.68^{+0.14}_{-0.16}$ signal fraction using the leading jet E_T distribution. (Right) A summary of CDF $t\bar{t}$ production cross section. The band is the theory expectation [1]

data for background processes to extract the $t\bar{t}$ total cross section of $6.0 \pm 1.6(\text{stat}) \pm 1.2(\text{syst})^1$ pb. Results of other $t\bar{t}$ production cross section measurements at CDF are summarized in Fig. 1 (Right).

2.2 Mass measurement

CDF has been exploring several different techniques for the top mass (m_t) measurement. The best single measurement shown in Fig. 2 (Left) is from a dynamic likelihood technique in the lepton+jets channel. The likelihood is defined as the differential cross section as a function of m_t per unit phase volume of the final partons multiplied by the transfer function from jets to parton quantities. The method takes into account all possible jet-parton and neutrino momentum assignments, and the likelihood is multiplied event by event. From the maximum likelihood analysis, the top mass is $177.8^{+4.5}_{-5.0} \pm 6.2$ GeV/ c^2 using 162 pb $^{-1}$ data. Results of other top mass measurements at CDF are shown in Fig. 2 (Right).

2.3 Single top search

Within the SM, top quarks are also expected to be produced singly by the electroweak interaction involving a Wtb vertex [2]. The measurement of the single top cross section is particularly interesting because the production cross section is proportional to $|V_{tb}|^2$, where V_{tb} is the Cabibbo-Kobayashi-Maskawa (CKM) matrix element which relates top and bottom quarks. At the Tevatron, the two relevant production modes are the t- and the s-channel exchange of a

¹Throughout the paper, the first error is statistical and the second is systematic unless otherwise specified.

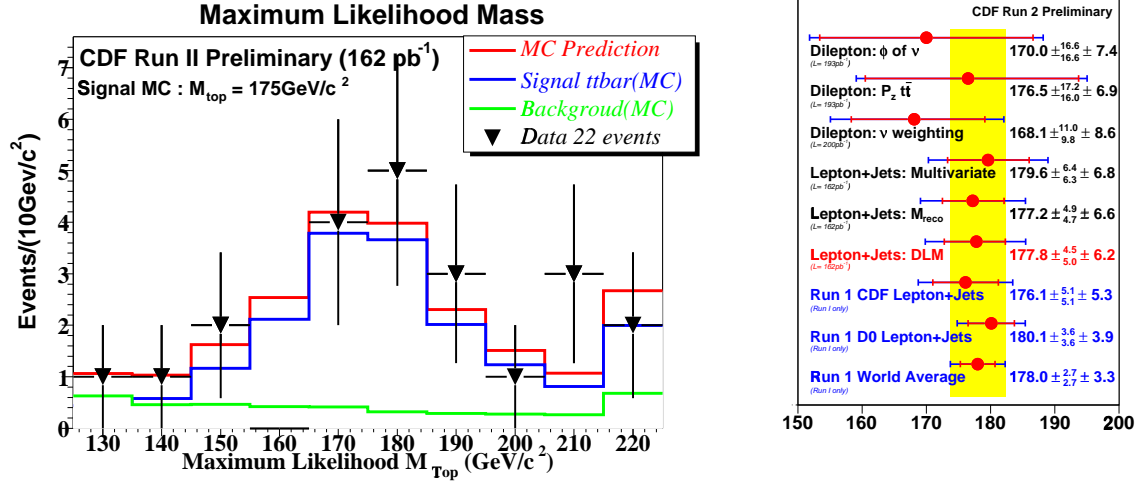


Figure 2: (Left) The maximum likelihood mass distributions in data and Monte Carlo. The signal Monte Carlo sample is for $m_t = 175 \text{ GeV}/c^2$. The first (last) bin includes under (over) flow. (Right) The summary of CDF top mass measurements. The band is the combined average.

virtual W boson. We find no significant evidence for electroweak top quark production in 162 pb^{-1} and set upper limits at the 95% confidence level on the production cross section, consistent with the SM prediction [1]: 10.1 pb for the t-channel, 13.6 pb for the s-channel and 17.8 pb for the combined cross section of t- and s-channel.

3 Beauty Physics

The beauty (B) physics program in CDF Run II is very competitive due to precision tracking and the silicon vertex trigger (SVT) which uses the impact parameters (d_o) of tracks. Three main triggers are used for B physics. The dilepton trigger is optimized for J/ψ , selecting either muon pairs or electron pairs. The SVT+lepton trigger selects one lepton of $p_T > 4 \text{ GeV}/c$ and one displaced track ($120 \mu\text{m} < d_o < 1 \text{ cm}$) with $p_T > 2 \text{ GeV}/c$ optimized for the semi-leptonic B decays. The two track trigger selects displaced track pairs with $p_T > 2 \text{ GeV}/c$ providing samples of fully hadronic B decays.

The B physics goals of CDF Run II include observation of B_s mixing and measurement of Δm_s , observation of CP violation and measurements of the CP asymmetries in golden b-decay modes, which is described in other papers of this proceedings by S. Menzemer. In this section, we instead present recent measurements of the inclusive b-hadron cross section, branching fractions, B baryon masses and lifetimes.

3.1 B Cross section and branching fraction

The Run I central b production cross section results, which included only b hadrons with $P_T > 5 \text{ GeV}/c$, were more than a factor of two greater than NLO QCD predictions [3, 4]. Dozens of

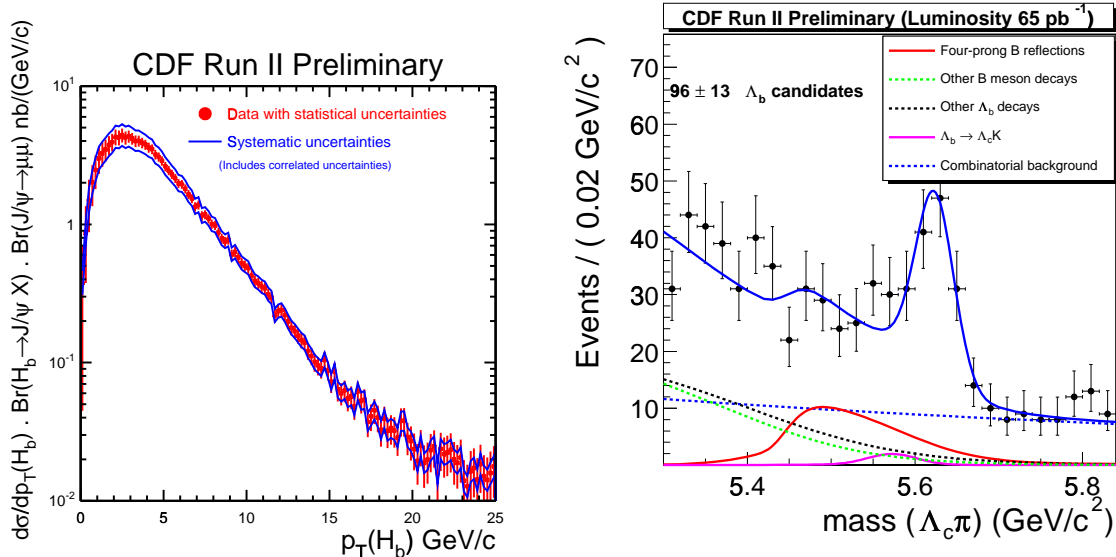


Figure 3: (Left) The differential $H_b \rightarrow J/\psi X$ production cross section as a function of $p_T(H_b)$. (Right) The invariant mass distribution of $\Lambda_b \rightarrow \Lambda_c^+ \pi^-$.

theoretical explanations were offered: NNLO corrections were large, intrinsic k_T effects are large, extreme value of the renormalization scales are required, new methods of resummation and fragmentation were required [5, 6]. These theories can broadly be categorized as “size” theories and “shape” theories. An inclusive measurement of bottom quark production over all transverse momenta can help resolve this ambiguity.

Using 37 pb^{-1} of the Run II J/ψ data sample, a measurement of the inclusive b-hadron production cross section in the decay channel $H_b \rightarrow J/\psi X$ is performed, where H_b denotes all b-hadrons that decay to J/ψ . The b-fraction is extracted using an unbinned likelihood fit to the proper decay length of the J/ψ in bins of $p_T(J/\psi)$ for $p_T(J/\psi) > 1.5$ GeV/c. The b-fractions obtained are applied to the measurement of the inclusive J/ψ cross section to obtain a measurement of the differential $H_b \rightarrow J/\psi X$ production cross section as a function of $p_T(J/\psi)$ shown in Fig. 3 (Left). The first measurement of the total b-hadron cross section at a hadronic machine has been extracted from the measurement of the cross section with $1.25 < p_T(J/\psi) < 17.0$ GeV/c using a Monte Carlo modeling of the decay kinematics of b hadrons to charmonium. We find $\sigma(p\bar{p} \rightarrow H_b X, |y| < 0.6) \cdot Br(H_b \rightarrow J/\psi X) \cdot Br(J/\psi \rightarrow \mu\mu) = 24.5 \pm 0.5 \pm 4.7$ nb. The total single b-quark cross section integrated over one unit of rapidity is $\sigma(p\bar{p} \rightarrow \bar{b} X, |y| < 1.0) = 29.4 \pm 0.6 \pm 6.2$ μ b.

A combination of the increased luminosity of Run II and new triggers oriented toward B-physics creates new opportunities to study the heavy baryons and expand our knowledge of the structure of baryonic matter. For an example, we observe 96 ± 13 events for the decay mode $\Lambda_b \rightarrow \Lambda_c^+ \pi^-$ using 65 pb^{-1} of data taken with the two track trigger. Fig. 3 (Right) shows a one-dimensional binned extended likelihood fit taking into account all possible reflections from B meson decays, and satellite contributions from both B mesons and other baryons. Using the signal, we measure $(f_{\Lambda_b}/f_d)(Br(\Lambda_b \rightarrow \Lambda_c^+ \pi^-)/Br(\bar{B}^0 \rightarrow D^+ \pi^-)) = 0.66 \pm 0.11 \pm 0.09 \pm 0.18$ and $Br(\Lambda_b \rightarrow \Lambda_c^+ \pi^-) = (6.0 \pm 1.0 \pm 0.8 \pm 2.1) \times 10^{-3}$ using other known quantities from PDG [9].

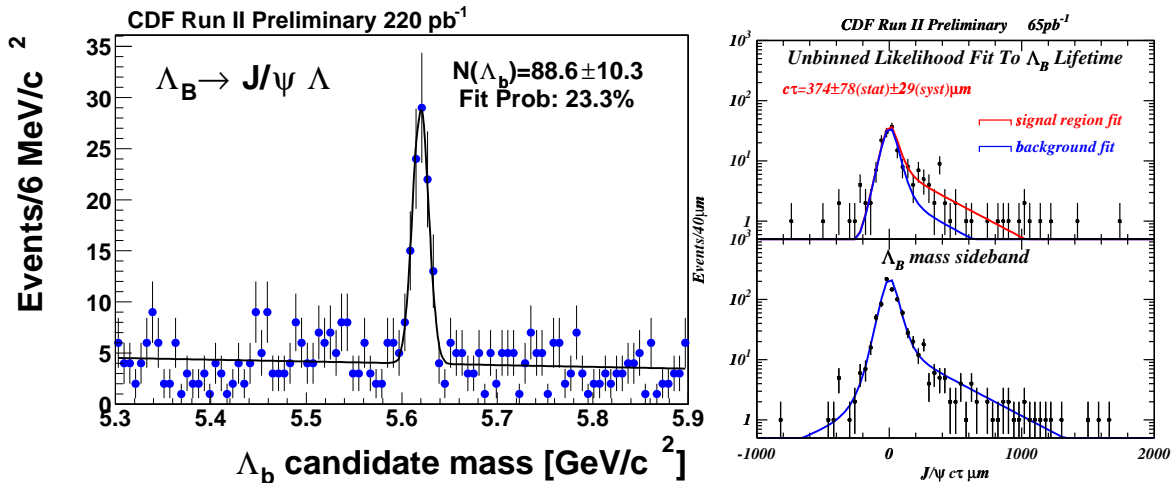


Figure 4: (Left) The invariant mass distribution of $\Lambda_b \rightarrow J/\psi \Lambda$ candidate events. (Right) A unbinned likelihood fit to Λ_b lifetime.

3.2 B baryon Masses and Lifetimes

We performed precision measurements of the mass of b-hadrons in exclusive J/ψ decay modes. The measured value of the Λ_b mass of the fully reconstructed decay to $J/\psi \Lambda$, is $m(\Lambda_b) = 5619.7 \pm 1.2 \pm 1.2 \text{ MeV}/c^2$, which is consistent with the CDF Run I measurement resolving a discrepancy in the PDG average. Figure 4 (Left) shows the invariant mass distribution of $\Lambda_b \rightarrow J/\psi \Lambda$ candidates in a data sample of 220 pb^{-1} .

We also measure the Λ_b lifetime in the exclusive decay modes $\Lambda_b \rightarrow J/\psi \Lambda$ where $J/\psi \rightarrow \mu^+ \mu^-$, $\Lambda \rightarrow p \pi^-$. Measuring the lifetime in this mode is particularly interesting since no measurement yet exists in a fully reconstructed mode. Many semi-leptonic measurements can claim only to be a measurement of the average b-baryon lifetime. Using 46 ± 9 reconstructed events in a sample of 65 pb^{-1} , the measured lifetime is $c\tau(\Lambda_b) = 374 \pm 78 \pm 29 \mu\text{m}$, shown in Fig. 4 (Right).

4 Charm Physics

Charm quarks are copiously produced at the Fermilab Tevatron. We reported on measurements of differential cross sections $d\sigma/dp_t$ for prompt charm meson production using $5.8 \pm 0.3 \text{ pb}^{-1}$ of data [10]. The data were also collected with the two track trigger. The charm meson cross sections were measured in the central rapidity region $|y| < 1$ with $P_T > 5.5 \text{ GeV}/c$ in four fully reconstructed decay modes: $D^0 \rightarrow K^- \pi^+$, $D^{*+} \rightarrow D^0 \pi^+$, $D^+ \rightarrow K^- \pi^+ \pi^+$, $D_s^+ \rightarrow \phi \pi^+$ and their charge conjugates. The measured differential cross sections are higher than theoretical predictions [11] by about 100% at low p_T and 50% at high p_T , however, they are compatible within uncertainties.

Large statistics of charm-enriched samples collected by CDF also provided opportunities for exploiting detailed features of charm decays such as D^+ Dalitz properties, the branching fraction of $D^+ \rightarrow \pi^+ \pi^- \pi^+$ and the properties of D^{**} . Using 210 pb^{-1} of data, we measure

masses of excited D -mesons, $M(D_1) - M(D^*) = 411.7 \pm 0.7 \pm 0.4 \text{ MeV}/c^2$ and $M(D_2) - M(D^*) = 594.0 \pm 0.6 \pm 0.5 \text{ MeV}/c^2$, as well as their widths, $\Gamma(D_1) = 20.5 \pm 1.7 \pm 1.3 \text{ MeV}$ and $\Gamma(D_2) = 49.5 \pm 2.1 \pm 1.2 \text{ MeV}$. Identifying the secondary D^{**} mesons, we also measure the two first moments (m_1 and m_2) of the invariant mass-squared distribution of the charm-hadron system in semi-leptonic B decays, $m_1 = \langle m_{D^{**}}^2 \rangle = (5.83 \pm 0.16 \pm 0.08) (\text{GeV}/c^2)^2$ and $m_2 = \langle (m_{D^{**}}^2 - m_1)^2 \rangle = (1.30 \pm 0.69 \pm 0.22) (\text{GeV}/c^2)^4$.

Exploiting the high mass resolution of the CDF tracking system, the Cabibbo-suppressed decays $D^0 \rightarrow K^+K^-$, $D^0 \rightarrow \pi^+\pi^-$ and $D^\pm \rightarrow \pi^-\pi^+\pi^\pm$ are well separated from the much larger Cabibbo-favored decays. Accurate understanding of the tracking asymmetries allow us to search for direct CP violation in these decays by looking for an asymmetry in the decay rate of $C = 1$ and $C = -1$ mesons. With 123 pb^{-1} data, the measured direct CP asymmetries are $A_{CP}(D^0 \rightarrow K^+K^-) = 2.0 \pm 1.2 \pm 0.6$ and $A_{CP}(D^0 \rightarrow \pi^+\pi^-) = 1.0 \pm 1.3 \pm 0.6$.

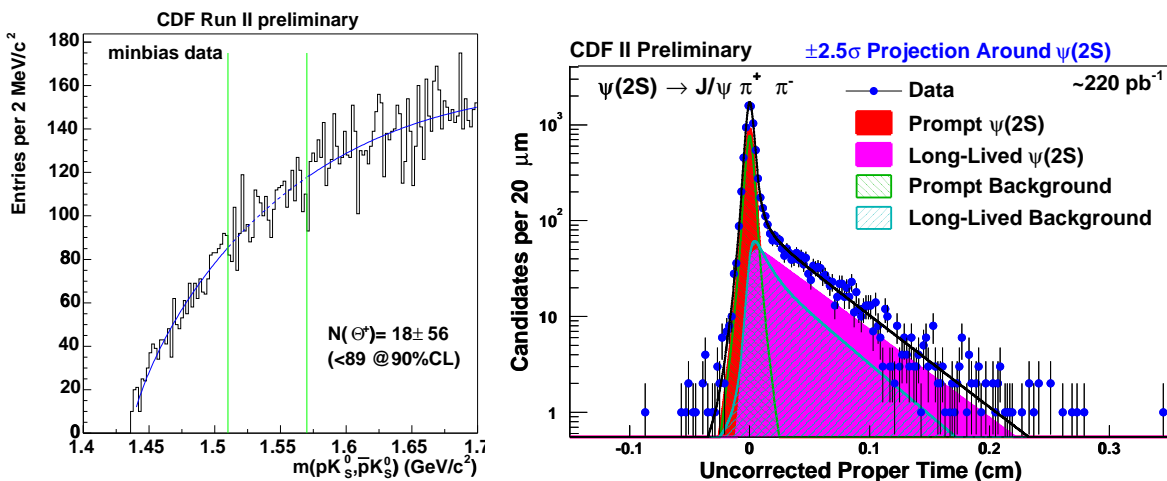


Figure 5: (Left) Invariant mass distribution of pK_S candidates from minimum bias data. The green lines indicate the signal region $1.510 \leq M(pK_S) \leq 1.570 \text{ GeV}/c$. (Right) The uncorrected proper-time projection of the $X(3872)$ likelihood probability density function.

5 Pentaquark search at CDF

Several experiments have reported evidence for pentaquark states, exotic baryons composed of 5 quarks, predicted in several models [7, 8]. A recent review [14] gives an excellent overview of the experimental status of pentaquarks, citing out ten reports of positive evidence and three reports of no observation. Using about 220 pb^{-1} , CDF found no evidence for the lightest pentaquark state $\Theta^+(uudd\bar{s})$ decaying to pK_S^0 . Figure 5 (Left) shows the invariant mass distribution of pK_S as an example of searches for the $\Theta^+ \rightarrow pK_S^0$. Earlier searches for the doubly strange pentaquarks ($\Xi_{3/2} \rightarrow \Xi^-\pi^\pm$) also yielded no signal, despite having an order of magnitude higher statistics in reference modes than the original evidence by NA49 [12]. CDF has also looked for charmed pentaquarks, reported by H1 [13], and no narrow resonances were found in $D^{*-}p$, D^-p or D^0p .

6 Properties of X(3872)

In 2003 the Belle collaboration reported the discovery of a narrow state, the X(3872), decaying to $J/\psi\pi^+\pi^-$ [15]. The CDF collaboration confirmed the $X(3872) \rightarrow J/\psi\pi^+\pi^-$ in about 220 pb^{-1} of $p\bar{p}$ collisions, and measured its mass with a value and precision similar to Belle [16]. The Belle observation demonstrates that B-decays can be a significant source of the X(3872), but otherwise its production rate in particle collisions is not known. Since this particle fits rather poorly into the charmonium framework, further studies of decay properties of X(3872) may offer insights of whether this new state has an exotic hadron quark composition.

To quantify the long-lived production component of the X(3872), we analyzed the lifetime distribution of $X(3872) \rightarrow J/\psi\pi^+\pi^-$. The Figure 5 (Right) shows the likelihood fit on uncorrected proper time for different parts of the lifetime. The fraction of long-lived X-signal that is measured to be $(16.1 \pm 4.9 \pm 2.0)\%$, in contrast to those produced promptly. For this sample with $p_T(J/\psi) \geq 4 \text{ GeV}/c$ production is dominated by prompt sources rather than b-decays.

References

- [1] R. Bonciani, S. Catani, M.L. Mangano and P. Nason, Nucl. Phys. B **529**, 424 (1998)
- [2] T. Stelzer *et al.*, Phys. Rev. D **56**, 5919 (1997); M.C. Smith and S.S. Willenbrock, Phys. Rev. D **54**, 6696 (1996); S. Mrenna and C.-P. Yuan, Phys. Lett. B **416**, 200 (1998).
- [3] F. Abe *et al.* (CDF), Phys. Rev. Lett. **75**, 1451 (1995)
- [4] D. Acosta *et al.* (CDF), Phys. Rev. **D65**, 052005 (2002)
- [5] M. Cacciari and P. Nason, Phys. Rev. Lett. **89**, 122003 (2002)
- [6] M. Cacciari, S. Frixione, M.L. Mangano, P. Nason, and G. Ridolfi, JHEP 0407, 033 (2004)
- [7] D. Diakonov, V. Petrov, and M.V. Polyakov, Z. Phys. **A359**, 305 (1997)
- [8] R.L. Jaffe and F. Wilczek, Phys. Rev. Lett. **91**, 232003 (2003)
- [9] K. Hagiwara *et al.* (Particle Data Group), Phys. Rev. **D66**, 010001 (2002)
- [10] D. Acosta *et al.* (CDF), Phys. Rev. Lett. **91**, 241804 (2003)
- [11] B.A. Kniehl, G. Kramer, and B. Potter, Nucl. Phys. **B597**, 337 (2001)
- [12] C. Alt *et al.* (NA49), Phys. Rev. Lett. **92**, 042003 (2004)
- [13] A. Aktas *et al.* (H1), Phys. Lett. **B588** 17 (2004)
- [14] Q. Zhao and F.E. Close, hep-ph/0404075 (2004)
- [15] S.-L. Choi *et al.* (Belle), Phys. Rev. Lett. **91**, 262001 (2003)
- [16] D. Acosta *et al.* (CDF), Phys. Rev. Lett. **93**, 072001 (2004)